ENVIRONMENTAL RESEARCH
LETTERS

PURPOSE-LED PUBLISHING™

LETTER • **OPEN ACCESS**

Black carbon in the Southern Andean snowpack

To cite this article: Raúl R Cordero *et al* 2022 *Environ. Res. Lett.* **17** 044042

IOP Publishing Environ. Res. Lett. 17 (2022) 044042 https://doi.org/10.1088/1748-9326/ac5df0

ENVIRONMENTAL RESEARCH
LETTERS

OPEN ACCESS

RECEIVED
29 August 2021

REVISED
2 March 2022

ACCEPTED FOR PUBLICATION
15 March 2022

PUBLISHED
25 March 2022

LETTER

Black carbon in the Southern Andean snowpack

Raúl R Cordero[1], Edgardo Sepúlveda[1], Sarah Feron[1,2,*], Chenghao Wang[3], Alessandro Damiani[1,4], Francisco Fernandoy[5], Steven Neshyba[6], Penny M Rowe[7], Valentina Asencio[8], Jorge Carrasco[9], Juan A Alfonso[10], Shelley MacDonell[11], Gunther Seckmeyer[12], Juan M Carrera[10], Jose Jorquera[1], Pedro Llanillo[13], Jacob Dana[14], Alia L Khan[14,15] and Gino Casassa[8]

[1] Universidad de Santiago de Chile. Av. Bernardo O'Higgins 3363, Santiago, Chile
[2] University of Groningen, 8911 CE, Leeuwarden, The Netherlands
[3] Department of Earth System Science, Stanford University, Stanford, CA 94305, United States of America
[4] Center for Environmental Remote Sensing, Chiba University, 1-33 Yayoicho, Inage Ward, Chiba 263-8522, Japan
[5] Universidad Andrés Bello, 980, Viña del Mar, Quillota, Chile
[6] Department of Chemistry, University of Puget Sound, 1500 N Warner St, Tacoma, WA, United States of America
[7] NorthWest Research Associates, Redmond, WA, United States of America
[8] Select Carbon Pty Ltd, Perth, WA, 6000, Australia
[9] University of Magallanes, Av. Manuel Bulnes 1855, Punta Arenas, Chile
[10] Instituto Venezolano de Investigaciones Cientificas (IVIC), Apartado 20632, Caracas, Venezuela
[11] Centro de Estudios Avanzados en Zonas Áridas (CEAZA), La Serena, Chile
[12] Leibniz Universität Hannover, Herrenhauser Strasse 2, Hannover, Germany
[13] Alfred Wegener Institute (AWI), Am Handelshafen 12, 27570 Bremerhaven, Germany
[14] Western Washington University, 516 High St, Bellingham, WA 98225, United States of America
[15] National Snow and Ice Data Center, Cooperative Institute for Research in Environmental Sciences, University of Colorado—Boulder, Boulder, CO, United States of America
[*] Author to whom any correspondence should be addressed.

E-mail: s.c.feron@rug.nl

Keywords: snow, black carbon, Andes

Supplementary material for this article is available online

Abstract

The Andean snowpack is an important source of water for many communities. As other snow-covered regions around the world, the Andes are sensitive to black carbon (BC) deposition from fossil fuel and biomass combustion. BC darkens the snow surface, reduces the albedo, and accelerates melting. Here, we report on measurements of the BC content conducted by using the meltwater filtration (MF) technique in snow samples collected across a transect of more than 2500 km from the mid-latitude Andes to the southern tip of South America. Addressing some of the key knowledge gaps regarding the effects of the BC deposition on the Andean snow, we identified BC-impacted areas, assessed the BC-related albedo reduction, and estimated the resulting snow losses. We found that BC concentrations in our samples generally ranged from 2 to 15 ng g^{-1}, except for the nearly BC-free Patagonian Icefields and for the BC-impacted sites nearby Santiago (a metropolis of 6 million inhabitants). We estimate that the seasonal snowpack shrinking attributable to the BC deposition ranges from 4 mm water equivalent (w.e.) at relatively clean sites in Patagonia to 241 mm w.e. at heavily impacted sites close to Santiago.

1. Introduction

The Andean snow cover is rapidly decreasing (Aguirre *et al* 2018, Malmros *et al* 2018, Saavedra *et al* 2018, Cordero *et al* 2019, Masiokas *et al* 2020), which has important implications for Andean countries. The Andes span more than 7000 km along western South America and their snowpack is an important source of water for many communities. Streams from meltwater in the tropical and mid-latitude Andes are particularly important for water supply, power generation, and agriculture (Vuille *et al* 2018, Berrouet *et al* 2020).

Although the interannual variability of precipitations in the Andean region is influenced by large-scale modes such as the El Niño-Southern Oscillation

(Cordero *et al* 2019, Masiokas *et al* 2020), decreasing snow trends in the mid-latitude Andes and Patagonia are likely driven by persistent increases in surface air temperature (Burger *et al* 2018, Saavedra *et al* 2018) and decreases in precipitation (Saavedra *et al* 2018, Cordero *et al* 2019). In the mid-latitude Andes, the negative trend in precipitation (Boisier *et al* 2018, Damiani *et al* 2020) is associated with a trend toward the positive phase of the southern annular mode (SAM) (Marshall 2003). SAM is the leading large-scale mode of atmospheric variability in the Southern Hemisphere south of 30° S (Thompson and Wallace 2000) and reflects the strength and position of the westerly winds (Fogt and Marshall 2020). During its positive phase, the westerlies weaken around 40° S, thus reducing precipitation in mid-latitudes. The trend toward the positive phase of the SAM, observed from the late 1950s to the early 2000s (Banerjee *et al* 2020), resulted in negative trends in both precipitation (Boisier *et al* 2018, Damiani *et al* 2020) and snow persistence for the southern Andes and Patagonia (Aguirre *et al* 2018, Malmros *et al* 2018, Saavedra *et al* 2018, Cordero *et al* 2019).

The snowpack in the Andean region may also be affected by aerosols and aerosol deposition. Some atmospheric aerosols scatter solar radiation back to space (Andreae *et al* 2005). The resulting cooling effect has partially counteracted the warming caused by the build-up of greenhouse gases (Storelvmo *et al* 2016). However, darker aerosols, such as black carbon (BC), absorb solar radiation causing the atmosphere to warm, and can also affect cloud formation and precipitations (Ramanathan and Carmichael 2008, Liu *et al* 2020). BC, commonly referred to as soot, is produced during combustion in diesel engines, coal burning, and residential wood burning, and wildfires (Bond *et al* 2013). These particles can be transported by near-surface winds flowing from the valleys west of the Andes towards the mountains (Sinclair and MacDonell 2021, Alfonso *et al* 2019, Gramsch *et al* 2020, Barraza *et al* 2021). The prevailing circulation in mid-latitude Andean mountains (mainly westerly airflow) (Garreaud 2009) favors particle transport/dispersion from sources in the Chilean valleys to the Andes.

Evidence of BC deposition has been found in Andean snow samples collected close to Santiago (a major city of 6 million inhabitants) and in the Atacama Desert (which hosts several major copper mines) (Alfonso *et al* 2019, Rowe *et al* 2019). BC darkens the snow, reduces the albedo (increasing the fraction of solar energy absorbed) and accelerates melting (Warren 2019, Kang *et al* 2020). BC has been found (although at concentrations much lower than in source regions) in snow samples in Antarctica (Warren and Clarke 1990, Casey *et al* 2017, Khan *et al* 2018, 2019, Kinase *et al* 2020, Cordero *et al* 2022), the Arctic (Clarke and Noone 2007, Doherty *et al* 2010, Dang *et al* 2017, Schulz *et al* 2018), North America (Doherty *et al* 2014, 2016, Khan *et al* 2017, Nagorski *et al* 2019), Northern China (Wang *et al* 2013), the Himalayas (Khan *et al* 2020, Usha *et al* 2021), and the Tibetan Plateau (Zhang *et al* 2018, Li *et al* 2019). While the low BC content in the Antarctic snow (generally lower than 5 ng g^{-1}) does not lead to major albedo reductions, the much higher BC concentrations found in samples from the Tibetan Plateau (often higher than 100 ng g^{-1}) can considerably affect the snow persistence by reducing the albedo by up to 0.2 (Zhang *et al* 2018).

Although the presence of BC has also been confirmed in the tropical Andes (Schmitt *et al* 2015, Soto Carrión *et al* 2021) and the mid-latitude Andes (Rowe *et al* 2019), no effort has so far targeted the southern Andes and Patagonia (latitudes higher than 42° S). There is also a gap in our knowledge of the albedo reduction, the resulting radiative forcing, and snow losses attributable to the BC deposition on the Andean snow. Here, we report on the first comprehensive survey of the BC content in seasonal snow in the southern Andes and Patagonia. We sampled across a transect of more than 2500 km including the Patagonian Icefields, which stretch over hundreds of kilometers atop the Andes Mountain range and are the southern hemisphere's largest expanses of ice outside of Antarctica. Our survey allowed us to address some of the key knowledge gaps regarding the effects of the BC deposition on the Andean snow.

2. Methods

2.1. Sample collection

A total of 279 samples were collected in 2017 and 2018 at 20 sites, relatively close to the local freezing level or zero-degree isotherm, across a transect of more than 2500 km from the mid-latitude Andes (Portillo, 32° S) to the southern tip of South America (Patagonia, Tierra del Fuego, 54° S) (figure 1). Surveys were generally carried out in late winter and early spring, at the beginning of the melt seasons; see table S1 (available online at stacks.iop.org/ERL/17/044042/mmedia) for further details. Snow sampling included the Patagonian Icefields, which stretch over hundreds of kilometers atop the Andes Mountains from latitude 46° S to latitude 51° S and are the Southern Hemisphere's largest expanses of ice outside of Antarctica (Dussaillant *et al* 2019).

As our aim was to assess the BC-related albedo reduction on a regional scale, sampling was conducted hundreds of meters away from BC sources such as towns and roads. A stainless-steel spatula was used to prevent contamination of snow at the sampling site (figure 1(b)). Samples were placed into plastic bags (figure 1(c)) and transported by using insulated coolers. Snowpits through the entire snowpack (up to 1 m depth) allowed us to study the vertical distribution of BC. At each site, we collected samples and measured

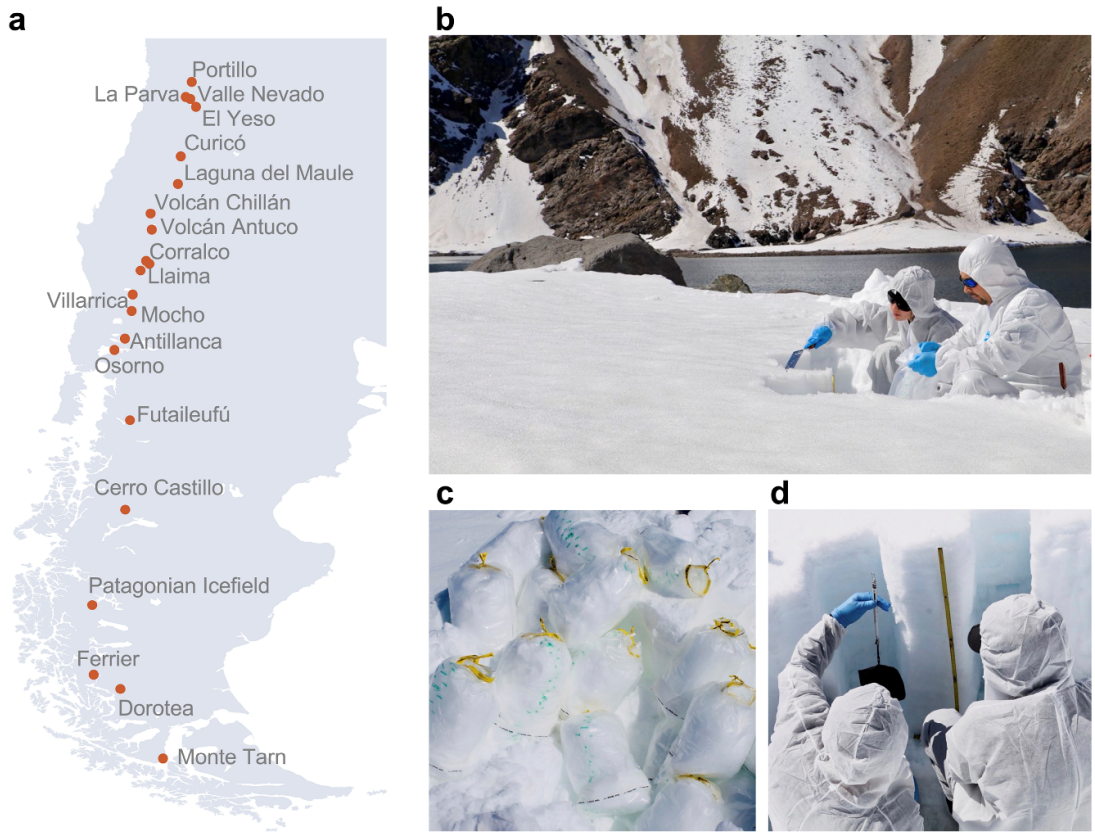

Figure 1. (a) Sampling sites. Since we aim to assess the effect of BC in the snow that affect the albedo on a regional scale, sampling was conducted hundreds of meters from apparent BC sources such as towns and roads. (b) Sampling at Portillo (the 'Laguna del Inca' lake appears in the background). A stainless-steel spatula was used to prevent contamination of snow at the sampling site. We generally sampled at the end of the accumulations season. (c) Samples were placed into plastic bags and transported by using insulated coolers; 279 samples were collected for this study. (d) Snowpits through the snowpack allowed us to study the accumulation of BC deposition though the season. We sampled at intervals of 10 cm depth from the surface and typically two parallel vertical profiles were collected. The density of the snow was also measured. Plots were generated by using Python's Matplotlib Library (Hunter 2007). Photographs taken by the authors. Informed consent was obtained for publication of identifying information/images in an online open-access publication.

the snow density at intervals of about 10 cm depth from the surface. Typically, two parallel vertical profiles were collected (figure 1(d)).

2.2. BC concentration, Angström exponent, and BC load

We applied the meltwater filtration (MF) technique (Clarke and Noone 2007, Grenfell *et al* 2011, Doherty *et al* 2013), which has been broadly applied for measuring BC concentrations in snow samples from the Arctic (Clarke and Noone 2007, Doherty *et al* 2010, Dang *et al* 2017), North America (Doherty *et al* 2014, 2016), Northern China (Wang *et al* 2013), the Andes (Rowe *et al* 2019), and Antarctica (Warren and Clarke 1990, Cordero *et al* 2022).

Following the procedure proposed Grenfell *et al* (2011), the MF technique required filtering the sample meltwater and measuring the spectral transmittance (340–750 nm) of the light through the filters. Calibration curves allowed us to translate the measured spectral transmittance into two related wavelength-dependent parameters: the BC-equivalent loading (L) and absorption optical depth (AOD). Since absorption by non-BC particles (such as dust) is generally negligible at wavelengths longer than 700 nm (Grenfell *et al* 2011), the BC concentration of each sample was computed from L values over the range 700–750 nm. In addition, the absorption Angström exponent (α) was computed by fitting the wavelength-dependent light absorption to a power law over the range 340–700 nm.

The total BC load within the snowpack (in units of mg m^{-2}) was calculated by multiplying the BC concentration (ng g^{-1}, averaged vertically through the snowpit) by the snow density (g m^{-3}, averaged vertically through the snowpit), and by the snowpack depth (m). For each site, we reported the mean of the values corresponding to the available vertical profiles (typically, two parallel vertical profiles were collected at each site; see figure 1(d)).

2.3. Albedo reduction, radiative forcing, and snowmelt

In order to estimate the albedo reduction (ΔA) attributable to BC deposition, we adopted the parameterization proposed by Dang *et al* (2015) and Dang

et al (2017)). Prior efforts have shown that larger albedo reductions generally result not only from high BC concentrations, but also from larger snow grains (Flanner *et al* 2007) and persistent cloudy conditions (Dang *et al* 2017).

According to Dang *et al* (2017), the all-sky broadband albedo reduction (ΔA) depends on cloud fraction (CF) and on the albedo reductions under overcast (ΔA_{cloudy}) and cloudless conditions (ΔA_{clear}). Estimates of ΔA_{cloudy} and ΔA_{clear} were retrieved from figure S1 (previously computed according to Dang *et al* (2015)) using the snow grain radii and the BC concentrations measured at the sampling sites. For CF, we used winter estimates (June, July, and August, or JJA) from the ERA5 atmospheric reanalysis (Hersbach 2016) averaged over the period 1981–2019.

In order to estimate the radiative forcing resulting from the BC deposition on seasonal snow, the corresponding albedo reduction (ΔA) was multiplied by the all-sky irradiance (I) at every sampling site. For I, we used JJA estimates from the ERA5 atmospheric reanalysis (Hersbach 2016) averaged over the period 1981–2019. The amount of extra energy (E_x) absorbed by the snowpack during winter (JJA) was computed by multiplying the BC-related radiative forcing by the number of winter days. Then, the snow (W) that melts sooner per unit of surface (due to the BC-related albedo reduction) in zones close to the zero-degree isotherm was estimated diving E_x by the latent heat of fusion (i.e. the energy needed to melt 1 kg of snow (Cohen 1994)).

2.4. Back-trajectory analysis

For selected sites, we computed 72 h backward trajectories for JJA days over the period 2010–2020 by applying the Hybrid Single-Particle Lagrangian Integrated Trajectory model (Draxler and Rolph 2015, Stein *et al* 2015). As inputs, we used data from the Global Data Assimilation System archive (NOAA Air Resources Laboratory (ARL) 2004). A cluster analysis based on the total spatial variance (Su *et al* 2015) was applied to the backward trajectories.

3. Results

3.1. BC concentration

Figure 2(a) suggests a latitude dependence of BC content in the snow samples. The BC concentration in snow samples from central Chile (32° S–36° S) ranged from 4 to 14 ng g^{-1} (corresponding to the 25th and 75th percentiles of all samples in this region), except for the sites close to Santiago (La Parva and Valle Nevado) where BC concentration ranged from 27 to 105 ng g^{-1}. BC decreased continuing south; BC concentration in southern Chile (36° S–42° S) ranged from 3 to 8 ng g^{-1}. The BC content in samples collected in central and southern Chile (36° S–42° S) approximately agrees with prior BC measurements that we conducted in the region in 2015 and 2016 (Rowe *et al* 2019), which suggests a limited interannual variability.

BC concentrations further decreased southward; BC concentration in Patagonia (42° S–54° S) ranged from 2 to 4 ng g^{-1}, except for the case of the Southern Patagonian Icefield, where BC concentration ranged from 0.2 to 2 ng g^{-1}. Similarly low BC concentrations have previously been observed only in Antarctic snow (Warren and Clarke 1990, Cordero *et al* 2022) making the snow in the Southern Patagonian Icefield the cleanest in the world outside of Antarctica. Except for BC-impacted sites (such as La Parva and Valle Nevado) and the BC-free sites in Patagonia (such as the Southern Patagonian Icefield), the BC concentration found in our snow samples ranged from 2 to 15 ng g^{-1}.

3.2. Dust presence

Figure 2(b) also suggests a latitude dependence of absorption Angström exponent. This exponent characterizes spectral absorption properties of all impurities in snow. The two most common particles in snow are soot and crustal dust. Values of the absorption Angström exponent close to 1.1 indicate the prevalence of BC in the sample while values closer to 4 suggest the dominance of dust (Wang *et al* 2013). Under most conditions, BC dominates aerosol light absorption because it has a mass absorption coefficient that is several orders of magnitude greater than dust at visible wavelengths. The values of the Angström exponent of the particles in our samples (generally higher than 2; figure 2(b)) reveal the considerable contribution of dust to light absorption in Andean snow. The presence of dust is apparent in our filters (figure S2); the shades of brown of some filters indicate the role of dust in the light absorption, especially in central Chile. In contrast, the shades of gray that prevail in filters collected in southern Chile are compatible with the fact that southern Chile (36° S–42° S) is less dusty than central Chile (32° S–36° S).

The absorption Angström exponent in samples collected in central Chile was generally higher than 3, but gradually decreased southward to values close to 2 at sites around latitude 40° S (figure 2(b)). The decrease southward in the Angström exponent suggests that the role of dust in the light absorption is smaller in southern Chile than in central Chile (32° S–36° S). The absorption Angström exponent rebounded in Patagonia (42° S–54° S); values higher than 3 for the Angström exponent were again measured at the Southern Patagonia Icefields (figure 2(b)). This rebound is not only driven by greater abundance of dust in eastern Patagonia (Gassó and Torres 2019), but also by the lack of BC sources in the region. Since the absorption Angström exponent is an indicator of the relative contribution of dust to light-absorption, the relatively high values of the Angström exponent in samples collected in Patagonia underline the low BC deposition in the region.

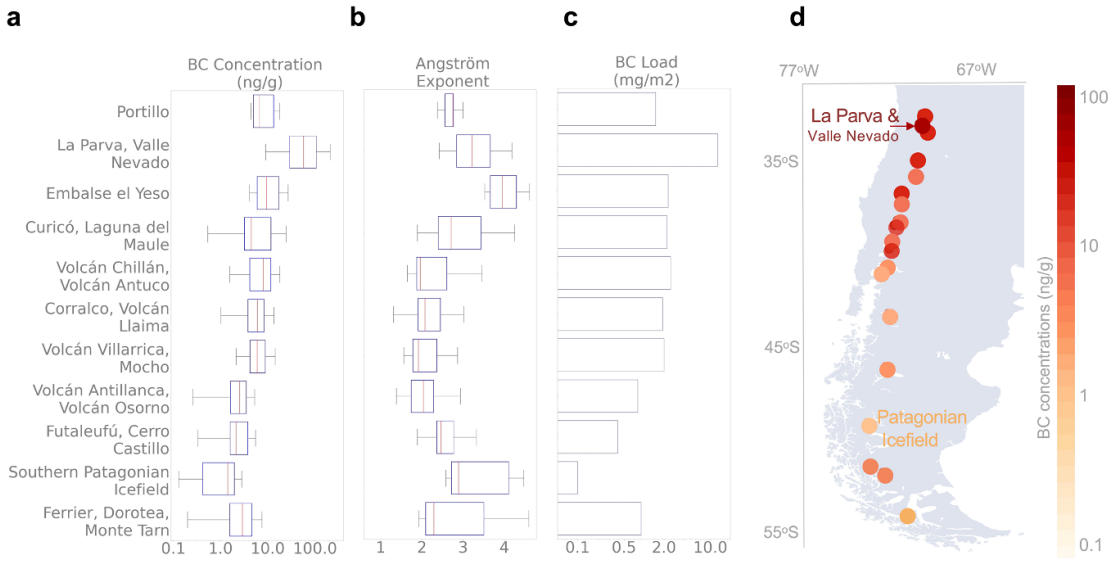

Figure 2. (a) Boxplot of the BC concentrations. (b) Boxplot of the absorption Angström exponent. (c) Barchart of the BC load measured through the entire snowpit. (d) Median of the BC concentrations found at the sampling sites. In central Chile (32° S–36° S), the BC concentration in the snow samples typically ranged from 4 to 14 ng g^{-1} (corresponding to the 25th and 75th percentiles of all samples in this region), excepting in the case of the sites close to Santiago (La Parva and Valle Nevado) where BC concentration approximately ranged from 27 to 105 ng g^{-1}. In southern Chile (36° S–42° S), BC concentration generally ranged from 3 to 8 ng g^{-1}. In Patagonia (42° S–54° S), the BC concentration in the snow samples typically ranged from 2 to 4 ng g^{-1}), except in the case of the Patagonian Icefield where BC concentration approximately ranged from 0.2 to 2 ng g^{-1}. Plots (a)–(c) may combine samples from nearby sites; see table S1 for details. Also note that each boxplot includes values obtained from samples collected through the entire snowpack at intervals of 10 cm depth from the surface. In each boxplot, the central mark (red stripe) indicates the median, and the edges indicate the 25th and 75th percentiles. The whiskers extend to the maximum and minimum data. Plots were generated by using Python's Matplotlib Library (Hunter 2007).

3.3. Total BC load

The BC load (figure 2(c)) measured through the entire snowpit was generally around 2 mg m^{-2} at sites in central Chile (32° S–36° S) and in southern Chile (36° S–42° S), where the population density generally ranges from 30 to 200 people per square kilometer (Sen 2021). However, in the case of the sites close to Santiago (the most populated city in the mid-latitude Andes with more than 6 million inhabitants), the BC load was about five times larger (around 10 mg m^{-2}); La Parva (33.36° S, 2600 m asl, figure S3(a)) is about 30 km East of Santiago (550 m asl) and is likely the most BC-impacted site in the southern Andes. The total BC amount within the snowpack decreased in Patagonia (42° S–54° S) to less than 1 mg m^{-2}; the lowest BC load was found in the Southern Patagonian Icefield (figure S3(b)), which is attributable to the fact that the Patagonian Icefields are far from any major BC source.

3.4. BC sources

Although wildfires are a prominent BC source in the Southern Hemisphere, their effect on winter (JJA) snow is likely minor. In the southern Andes and Patagonia, the climate is defined by the mid-latitude westerly regime that prevails year-round (Garreaud *et al* 2013). Westerly winds limit meridional airborne transport but enable long-range transport to the western Andes; smoke from bushfires in eastern Australia has been detected over Southern Patagonia (Ohneiser *et al* 2020).

Despite the episodic intercontinental BC transport, back-trajectory analysis suggests that most of the BC found in the western Andean snow was emitted in Chile (figure 3). For example, a majority of 72 h back-trajectories (61%) for La Parva and Valle Nevado passes over Santiago (see clusters 2 and 3 in figure 3(a)). Trajectories in the most frequent cluster are characterized by being short, with relatively low wind speeds (4 km h^{-1}). The second most frequent cluster of back-trajectories for La Parva and Valle Nevado comes from northern Chile, passing relatively close to Los Bronces (figure 3(a)).

In the case of sites in southern Chile (36° S–42° S), a majority of back-trajectories (see for example the case of Llaima; figure 3(b)) are characterized by slow air movement from the north. The second most frequent cluster of back-trajectories for sites in southern Chile suggests faster air movement passing over Chilean valleys, close to cities and towns. In the case of Southern Patagonian Icefield (figure 3(c)), the wind speeds of clusters 1 and 2 (accounting for 53% of the back-trajectories) are considerably strong as the southern tip of the continent dips into a belt of prevailing westerly winds. None of the 72 h back-trajectories computed for the Southern Patagonian Icefield passes over relevant BC sources.

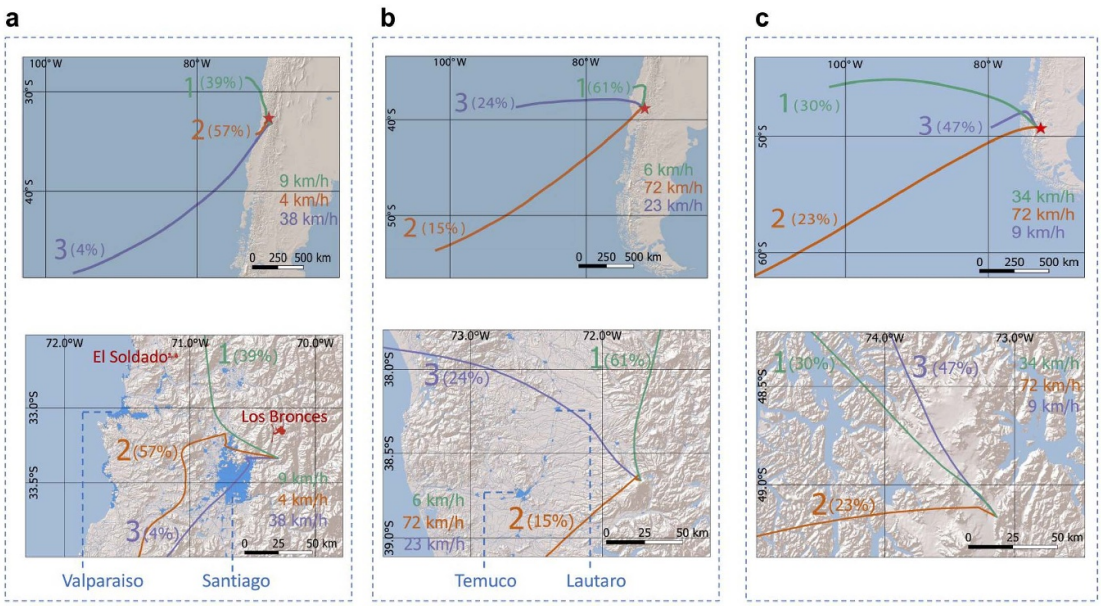

Figure 3. Clusters of 72 h backward trajectories for JJA days over the period 2010–2020. (a) La Parva (30 km East of Santiago); (b) Llaima (southern Chile); (c) Patagonian Icefield. Second row shows a close-up of plots in the first row. In the second row, the footprint of major mining projects and cities are highlighted in red and blue, respectively. According to Sen (2021), Santiago has a population of about 6 million residents, Valparaiso about 1 million, Temuco about 0.3 million, and Lautaro has about 50 000 residents. Polygon coordinates of mining projects were obtained from Maus *et al* (2020). Back-trajectory analysis suggests that most of the BC found in the western Andean snow was emitted in the Chilean valleys and transported by near-surface winds towards the mountains. Plots were generated using MeteoInfo software tools for meteorological data visualization (Wang 2014).

3.5. Albedo reduction and snow melt

The BC-content in snow samples reduces the snow albedo, which increases the fraction of solar energy absorbed and causes a positive radiative forcing. The BC-related forcing can be taken as the albedo reduction times the shortwave (SW) irradiance. For example, according to the parameterization by Dang *et al* (2017), the BC concentration in snow samples from central Chile (32° S–36° S), which ranges from 4 to 14 ng g^{-1}, reduces the snow albedo by 0.005–0.018 (figure S1). Considering that all-sky SW irradiance averaged for winter months (JJA) in central Chile is within the range 134–148 W m^{-2} (figures 4(a) and S4), an albedo reduction of 0.005–0.018 leads to a forcing of 0.7–2.7 W m^{-2} locally. Following the regional distribution of the BC burden (figure 2(a)), the forcing was greatest at the sites close to Santiago (the radiative forcing is estimated to be within the range 2.4–10 W m^{-2} at La Parva and Valle Nevado) and least at the Southern Patagonian Icefield; although frequent clouds in Patagonia (figure 4(b)) favor BC-related albedo reduction, the radiative forcing is estimated to be within the range 0–0.3 W m^{-2} at the Southern Patagonian Icefield. Albedo reductions attributable to BC deposition are shown for each sampling site in figure 4(c).

The forcing attributable to BC deposition accelerates melting of seasonal snow. For example, the albedo reduction of 0.018–0.07 estimated for La Parva and Valle Nevado makes the local snowpack absorb on average an extra of 19–80 MJ m^{-2} during winter. In a single sunny winter day, the extra solar energy absorbed by the snowpack at La Parva and Valle Nevado is within the range 0.3–1.2 MJ m^{-2}. This huge amount of energy may considerably accelerate melting of the snow below the 0 °C isotherm.

At heavily impacted sites such as La Parva and Valle Nevado, we estimate that the seasonal snow that melts sooner per unit of surface due to a BC-related albedo reduction is likely within the range 56–241 kg m^{-2}, which is equivalent to a snowpack shrinking of about 56–241 mm water equivalent (w.e.). Contrary, due to the relatively low BC load, we estimated that in Patagonia the snowpack reduction may amount only to 4–11 mm w.e., which is fortunately only equivalent to a small fraction of the seasonal precipitation in the region (figure S5). Table 1 shows our estimates of the seasonal snow that melts sooner due to the BC deposition for some regions of interest.

4. Discussion

Despite the importance of the Andean snowpack as source of water for many communities, prior to this work there were no measurements of BC deposition on the snow in the southern Andes and Patagonia. There were also large gaps in our knowledge of the albedo reduction and the resulting radiative effects and snow loss associated with BC deposition on Andean snow. Here, we report measurements of

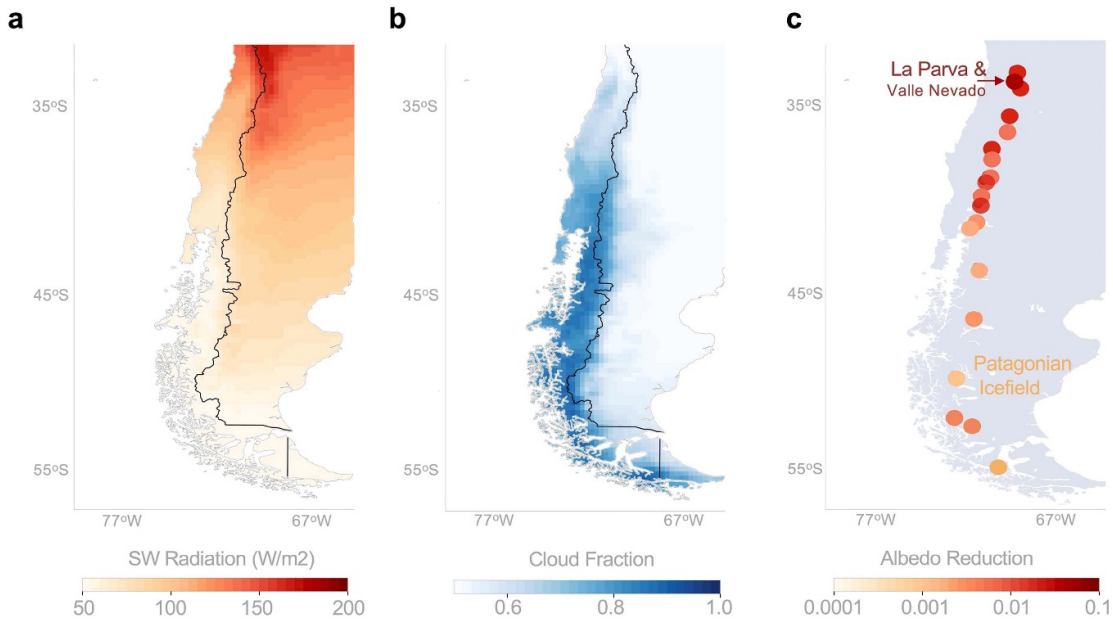

Figure 4. (a) Shortwave (SW) all-sky irradiance averaged for winter months (JJA) over the period 1981–2019. (b) Cloud fraction (CF) averaged for winter months (JJA) over the period 1981–2019. (c) Albedo reductions attributable to BC concentrations. Data from the ERA5 atmospheric reanalysis (Hersbach 2016) were used for plots (a) and (b). The parameterization by Dang *et al* (2015) was used for computing the albedo reduction in (c). Plots were generated by using Python's Matplotlib Library (Hunter 2007).

Table 1. Main results. From left to right: regions or sites of interest; BC concentrations correspond to the 25th and 75th percentiles of the BC measured in all samples in the regions or sites of interest; BC-related albedo reduction (ΔA) computed according to the parameterization proposed by Dang *et al* (2015) and (2017); winter (JJA) estimates of the SW irradiance for the regions (or sites) of interest; radiative forcing attributable to the BC deposition; extra energy absorbed by the snowpack during winter attributable to the BC deposition; snow that melts sooner due to local BC deposition. We have included in the supplementary material a step-by-step description of the calculations that rendered the snowmelt estimates.

Region or sites	BC concentration (ng g^{-1})	Albedo reduction (ΔA)	JJA SW irradiance (W m^{-2})	BC-related forcing (W m^{-2})	Extra energy absorbed (MJ m^{-2})	Snow melt (mm w.e.)
La Parva and Valle Nevado	27–105	0.018–0.07	134–148	2.4–10	19–80	56–241
Central Chile (32° S–36° S)	4–14	0.005–0.018	134–148	0.7–2.7	5.2–21	16–62
Southern Chile (36° S–42° S)	3–8	0.005–0.012	97–107	0.5–1.2	3.8–10.0	11–30
Patagonia (42° S–54° S)	2–4	0.003–0.008	51–59	0.2–0.5	1.2–3.7	4–11
Patagonian Icefield	0.2–2	0.0006–0.005	51–59	0–0.3	0–2.3	0–7

the BC content in the snowpack in southern Andes and Patagonia as well as estimates of the albedo reduction, radiative forcing, and snow losses attributable to the BC deposition.

The lowest BC concentration was measured in the Southern Patagonian Icefield. The fact that the southern tip of America dips into a belt of prevailing westerly winds, isolated from any major BC source, makes the snow in the region one of the cleanest in the world outside of Antarctica; BC concentrations as low as those measured in the Southern Patagonian Icefield (lower than 1 ng g^{-1}) have only been observed in Antarctic snow (Warren and Clarke 1990, Cordero *et al* 2022).

The maximum BC concentration was measured at sites close to Santiago, a metropolis of more than 6 million inhabitants. BC concentrations close to Santiago (La Parva and Valle Nevado) were at least one order of magnitude higher than those measured elsewhere in the southern Andean snowpack. BC concentrations in central Chile (32° S–36° S) were in general higher than those measured in southern Chile (36° S–42° S), which can be partially attributed to the higher snowfall rates in southern Chile. However, the total BC load (which provides an indication of the total BC deposited on the snowpack regardless of the snowfall rate) was comparable both in southern Chile (36° S–42° S) and in central Chile

(32° S–36° S). An exception was the BC load measured at La Parva and Valle Nevado, which was on average about five times larger than the BC load measured elsewhere in central and southern Chile. La Parva (30 km East of Santiago) is likely the most BC-impacted site in the southern Andes.

Excluding the BC-impacted sites close to Santiago and the nearly BC-free site in the Southern Patagonian Icefield, the BC concentration found in our snow samples ranged from 2 to 15 ng g^{-1} (corresponding to the 25th and 75th percentiles of all samples), which can be considered moderate values. Similar values have been observed in snow samples collected in Canada and in the US Pacific Northwest (Doherty *et al* 2014). Even the relatively high BC concentrations measured at sites close to Santiago (27–105 ng g^{-1}) are at least one order of magnitude lower than those measured in snow samples collected in northeastern China (Wang *et al* 2013).

Although BC concentrations in central and southern Chile are generally moderate, impacted areas are subjected to a considerable BC-related radiative forcing. At La Parva, for example, BC deposition reduces the albedo leading to a positive radiative forcing by up to 10 W m^{-2}. Attributable to the BC-related radiative forcing, we estimated that, in areas close to the zero-degree isotherm nearby La Parva, BC deposition can make the seasonal snowpack lose up to 241 mm w.e., which is a considerable fraction of the snow accumulation in the region.

The BC footprint of major cities like Santiago on the Andean snowpack was likely larger some decades ago before environmental policies began to be adopted in the country. For example, driven by air-quality regulations, the daily fine particle matter (PM2.5) fraction has dropped by approximately 60% during the last two decades in Santiago (Gramsch *et al* 2021). However, our results show that more remains to be done to reduce BC deposition on the Andean snowpack.

Data availability statements

All-sky shortwave irradiance, broadband albedo, cloud fraction (CF), and snowfall data were obtained over the period 1981–2019 from the ERA5 atmospheric reanalysis available at https://cds.climate.copernicus.eu/cdsapp#!/dataset/derived-near-surface-meteorological-variables?tab=overview. Our BC measurements are available at http://antarctica.cl/bc-data/.

The data that support the findings of this study are openly available at the following URL/DOI: http://antarctica.cl/bc-data/.

Author contributions

R R C, S F, A D, J C, G S, P M R, S N and A L K: wrote the main manuscript text. S F, E S C W and F F prepared figures. R R C, S F, E S, F F, V A, J A A, S M, J M C, J J, J D A L K, P L and G C collected and analyzed samples. All authors reviewed the manuscript.

Acknowledgments

The support of ANID (ANILLO ACT210046, FONDECYT 1191932, DFG190004 and REDES180158), and CORFO (Preis 19BP-117358, 18BPE-93920 and 18BPCR-89100) is gratefully acknowledged. A L K's contribution was supported by a Fulbright Scholarship to the Chilean Antarctic Program.

Author confirmation

The authors have confirmed that any identifiable participants in this study have given their consent for publication.

Conflict of interest

The authors declare no competing interests.

ORCID iDs

Raúl R Cordero https://orcid.org/0000-0001-7607-7993
Sarah Feron https://orcid.org/0000-0002-0572-5639
Chenghao Wang https://orcid.org/0000-0001-8846-4130

References

Aguirre F, Carrasco J, Sauter T, Schneider C, Gaete K, Garín E, Adaros R, Butorovic N, Jaña R and Casassa G 2018 Snow cover change as a climate indicator in Brunswick Peninsula, Patagonia *Front. Earth Sci.* **6** 130

Alfonso J A *et al* 2019 Elemental and mineralogical composition of the western Andean snow (18° S–41° S) *Sci. Rep.* **9** 1–13

Andreae M O, Jones C D and Cox P M 2005 Strong present-day aerosol cooling implies a hot future *Nature* **435** 1187–90

Banerjee A, Fyfe J C, Polvani L M, Waugh D and Chang K L 2020 A pause in Southern Hemisphere circulation trends due to the montreal protocol *Nature* **579** 544–8

Barraza F, Lambert F, MacDonell S, Sinclair K, Fernandoy F and Jorquera H 2021 Major atmospheric particulate matter sources for glaciers in Coquimbo region, Chile *Environ. Sci. Pollut. Res.* **28** 1–11

Berrouet L, Villegas-Palacio C and Botero V 2020 Vulnerability of rural communities to change in an ecosystem service provision: surface water supply. A case study in the Northern Andes, Colombia *Land Use Policy* **97** 104737

Boisier J P *et al* 2018 Anthropogenic drying in central-southern Chile evidenced by long-term observations and climate model simulations *Elem.: Sci. Anth.* **6** 1–20

Bond T C *et al* 2013 Bounding the role of black carbon in the climate system: a scientific assessment *J. Geophys. Res.: Atmos.* **118** 5380–552

Burger F, Brock B and Montecinos A 2018 Seasonal and elevational contrasts in temperature trends in central Chile between 1979 and 2015 *Glob. Planet. Change* **162** 136–47

Casey K A, Kaspari S D, Skiles S M, Kreutz K and Handley M J 2017 The spectral and chemical measurement of pollutants

on snow near South Pole, Antarctica *J. Geophys. Res.: Atmos.* **122** 6592–610
Clarke A D and Noone K J 2007 Soot in the Arctic snowpack: a cause for perturbations in radiative transfer *Atmos. Environ.* **41** 64–72
Cohen J 1994 Snow cover and climate *Weather* **49** 150–6
Cordero R R *et al* 2022 Black carbon footprint of human presence in Antarctica *Nat. Commun.* **13** 1–11
Cordero R R, Asencio V, Feron S, Damiani A, Llanillo P J, Sepulveda E, Jorquera J, Carrasco J and Casassa G 2019 Dry-season snow cover losses in the Andes (18° S–40° S) driven by changes in large-scale climate modes *Sci. Rep.* **9** 1–10
Damiani A, Cordero R R, Llanillo P J, Feron S, Boisier J P, Garreaud R, Rondanelli R, Irie H and Watanabe S 2020 Connection between Antarctic ozone and climate: interannual precipitation changes in the Southern Hemisphere *Atmosphere* **11** 579
Dang C, Brandt R E and Warren S G 2015 Parameterizations for narrowband and broadband albedo of pure snow and snow containing mineral dust and black carbon *J. Geophys. Res.: Atmos.* **120** 5446–68
Dang C, Warren S G, Fu Q, Doherty S J, Sturm M and Su J 2017 Measurements of light-absorbing particles in snow across the Arctic, North America, and China: effects on surface albedo *J. Geophys. Res.: Atmos.* **122** 10–149
Doherty S J, Dang C, Hegg D A, Zhang R and Warren S G 2014 Black carbon and other light-absorbing particles in snow of central North America *J. Geophys. Res.: Atmos.* **119** 12–807
Doherty S J, Grenfell T C, Forsström S, Hegg D L, Brandt R E and Warren S G 2013 Observed vertical redistribution of black carbon and other insoluble light-absorbing particles in melting snow *J. Geophys. Res.: Atmos.* **118** 5553–69
Doherty S J, Hegg D A, Johnson J E, Quinn P K, Schwarz J P, Dang C and Warren S G 2016 Causes of variability in light absorption by particles in snow at sites in Idaho and Utah *J. Geophys. Res.: Atmos.* **121** 4751–68
Doherty S J, Warren S G, Grenfell T C, Clarke A D and Brandt R E 2010 Light-absorbing impurities in Arctic snow *Atmos. Chem. Phys.* **10** 11647–80
Draxler R R and Rolph G D 2015 HYSPLIT (HYbrid Single-Particle Lagrangian Integrated Trajectory) model access via NOAA ARL READY website (NOAA Air Resources Laboratory, Silver Spring) (available at: http://ready.arl.noaa.gov/HYSPLIT.php)
Dussaillant I, Berthier E, Brun F, Masiokas M, Hugonnet R, Favier V, Rabatel A, Pitte P and Ruiz L 2019 Two decades of glacier mass loss along the Andes *Nat. Geosci.* **12** 802–8
Flanner M G, Zender C S, Randerson J T and Rasch P J 2007 Present-day climate forcing and response from black carbon in snow *J. Geophys. Res.: Atmos.* **112** D11
Fogt R L and Marshall G J 2020 The southern annular mode: variability, trends, and climate impacts across the Southern Hemisphere *Wiley Interdiscip. Rev. Clim. Change* **11** 1–24
Garreaud R D 2009 The Andes climate and weather *Adv. Geosci.* **22** 3–11
Garreaud R, Lopez P, Minvielle M and Rojas M 2013 Large-scale control on the Patagonian climate *J. Clim.* **26** 215–30
Gassó S and Torres O 2019 Temporal characterization of dust activity in the central Patagonia desert (years 1964–2017) *J. Geophys. Res.: Atmos.* **124** 3417–34
Gramsch E, Muñoz A, Langner J, Morales L, Soto C, Pérez P and Rubio M A 2020 Black carbon transport between Santiago de Chile and glaciers in the Andes Mountains *Atmos. Environ.* **232** 117546
Gramsch E, Oyola P, Reyes F, Rojas F, Henríquez A and Kang C M 2021 Trends in particle matter and its elemental composition in Santiago de Chile, 2011–2018 *J. Air Waste Manage. Assoc.* **71** 721–36
Grenfell T C, Doherty S J, Clarke A D and Warren S G 2011 Light absorption from particulate impurities in snow and ice determined by spectrophotometric analysis of filters *Appl. Opt.* **50** 2037–48
Hersbach H 2016 The ERA5 atmospheric reanalysis *AGUFM, 2016* pp NG33D–01
Hunter J D 2007 Matplotlib: a 2D graphics environment *IEEE Ann. Hist. Comput.* **9** 90–95
Kang S, Zhang Y, Qian Y and Wang H 2020 A review of black carbon in snow and ice and its impact on the cryosphere *Earth-Sci. Rev.* **210** 103346
Khan A L, Klein A G, Katich J M and Xian P 2019 Local emissions and regional wildfires influence refractory black carbon observations near Palmer Station, Antarctica *Front. Earth Sci.* **7** 49
Khan A L, McMeeking G R, Schwarz J P, Xian P, Welch K A, Berry Lyons W and McKnight D M 2018 Near-surface refractory black carbon observations in the atmosphere and snow in the McMurdo dry valleys, Antarctica, and potential impacts of foehn winds *J. Geophys. Res.: Atmos.* **123** 2877–87
Khan A L, Rittger K, Xian P, Katich J M, Armstrong R L, Kayastha R B, Dana J L and McKnight D M 2020 Biofuel burning influences refractory black carbon concentrations in seasonal snow at lower elevations of the Dudh Koshi River Basin of Nepal *Front. Earth Sci.* **8**
Khan A L, Wagner S, Jaffe R, Xian P, Williams M, Armstrong R and McKnight D 2017 Dissolved black carbon in the global cryosphere: concentrations and chemical signatures *Geophys. Res. Lett.* **44** 6226–34
Kinase T *et al* 2020 Concentrations and size distributions of black carbon in the surface snow of eastern Antarctica in 2011 *J. Geophys. Res.: Atmos.* **125** e2019JD030737
Li Y, Kang S, Chen J, Hu Z, Wang K, Paudyal R, Liu J, Wang X, Qin X and Sillanpää M 2019 Black carbon in a glacier and snow cover on the northeastern Tibetan Plateau: concentrations, radiative forcing and potential source from local topsoil *Sci. Total Environ.* **686** 1030–8
Liu L *et al* 2020 Impact of biomass burning aerosols on radiation, clouds, and precipitation over the Amazon: relative importance of aerosol–cloud and aerosol–radiation interactions *Atmos. Chem. Phys.* **20** 13283–301
Malmros J K, Mernild S H, Wilson R, Tagesson T and Fensholt R 2018 Snow cover and snow albedo changes in the central Andes of Chile and Argentina from daily MODIS observations (2000–2016) *Remote Sens. Environ.* **209** 240–52
Marshall G J 2003 Trends in the southern annular mode from observations and reanalyses *J. Clim.* **16** 4134–43
Masiokas M H *et al* 2020 A review of the current state and recent changes of the Andean cryosphere *Front. Earth Sci.* **8** 99
Maus V, Giljum S, Gutschlhofer J, da Silva D M, Probst M, Gass S L, Luckeneder S, Lieber M and McCallum I 2020 A global-scale data set of mining areas *Sci. Data* **7** 1–13
Nagorski S A, Kaspari S D, Hood E, Fellman J B and Skiles S M 2019 Radiative forcing by dust and black carbon on the Juneau Icefield, Alaska *J. Geophys. Res.: Atmos.* **124** 3943–59
NOAA Air Resources Laboratory (ARL) 2004 Global data assimilation system (GDAS1) archive information Tech. rep (available at: http://ready.arl.noaa.gov/gdas1.php)
Ohneiser K *et al* 2020 Smoke of extreme Australian bushfires observed in the stratosphere over Punta Arenas, Chile, in January 2020: optical thickness, lidar ratios, and depolarization ratios at 355 and 532 nm *Atmos. Chem. Phys.* **20** 8003–15
Ramanathan V and Carmichael G 2008 Global and regional climate changes due to black carbon *Nat. Geosci.* **1** 221–7
Rowe P M *et al* 2019 Black carbon and other light-absorbing impurities in snow in the Chilean Andes *Sci. Rep.* **9** 1–16
Saavedra F A, Kampf S K, Fassnacht S R and Sibold J S 2018 Changes in Andes snow cover from MODIS data, 2000–2016 *Cryosphere* **12** 1027–46
Schmitt C G, All J D, Schwarz J P, Arnott W P, Cole R J, Lapham E and Celestian A 2015 Measurements of light-absorbing particles on the glaciers in the Cordillera Blanca, Peru *Cryosphere* **9** 331–40
Schulz H, Fried N, Zanatta M, Maturilli M, Rapp J, Herber A and Gerdes R 2018 Spatial and temporal variability of black

carbon in snow measured with an SP2 around Ny-Alesund *European Geosciences Union General Assembly*

Sen O 2021 Largest cities in South America *World Atlas. World Facts* (available at: www.worldatlas.com) (Accessed January 2021)

Sinclair K E and MacDonell S 2016 Seasonal evolution of penitente glaciochemistry at Tapado Glacier, Northern Chile *Hydrol. Process.* **30** 176–86

Soto Carrión C, Schmitt C G, Zúñiga Negrón J J, Jiménez Mendoza W, Arbieto Mamani O, Pozo Enciso R S, Guevara Sarmiento S J and Rado Cuchills M S 2021 Quantitative estimation of black carbon in the glacier Ampay-Apurimac *J. Sustain. Dev. Energy Water Environ. Syst.* **9** 3–0

Stein A F, Draxler R R, Rolph G D, Stunder B J, Cohen M D and Ngan F 2015 NOAA's HYSPLIT atmospheric transport and dispersion modeling system *Bull. Am. Meteorol. Soc.* **96** 2059–77

Storelvmo T, Leirvik T, Lohmann U, Phillips P C and Wild M 2016 Disentangling greenhouse warming and aerosol cooling to reveal Earth's climate sensitivity *Nat. Geosci.* **9** 286–9

Su L, Yuan Z, Fung J C and Lau A K 2015 A comparison of HYSPLIT backward trajectories generated from two GDAS datasets *Sci. Total Environ.* **506** 527–37

Thompson D W J and Wallace J M 2000 Annular modes in the extratropical circulation. Part I: month-to-month variability *J. Clim.* **13** 1000–16

Usha K H, Nair V S and Babu S S 2021 Effect of aerosol-induced snow darkening on the direct radiative effect of aerosols over the Himalayan region *Environ. Res. Lett.* **16** 064004

Vuille M *et al* 2018 Rapid decline of snow and ice in the tropical Andes–impacts, uncertainties and challenges ahead *Earth-Sci. Rev.* **176** 195–213

Wang X, Doherty S J and Huang J 2013 Black carbon and other light-absorbing impurities in snow across Northern China *J. Geophys. Res.: Atmos.* **118** 1471–92

Wang Y Q 2014 MeteoInfo: GIS software for meteorological data visualization and analysis *Meteorol. Appl.* **21** 360–8

Warren S G 2019 Light-absorbing impurities in snow: a personal and historical account *Front. Earth Sci.* **6** 250

Warren S G and Clarke A D 1990 Soot in the atmosphere and snow surface of Antarctica *J. Geophys. Res.: Atmos.* **95** 1811–6

Zhang Y *et al* 2018 Black carbon and mineral dust in snow cover on the Tibetan Plateau *Cryosphere* **12** 413–31